Extracting phytoplankton physiological traits from batch and chemostat culture data

A. W. Omta,[1]* D. Talmy,[1] D. Sher,[2] Z. V. Finkel,[3] A. J. Irwin,[3] M. J. Follows[1]

[1]Department of Earth, Atmospheric and Planetary Sciences, Massachusetts Institute of Technology, Cambridge, Massachusetts
[2]Department of Marine Biology, Leon H. Charney School of Marine Sciences, University of Haifa, Mount Carmel, Haifa, Israel
[3]Department of Math and Computer Science, Sackville, New Brunswick, Canada

Abstract

As the role of phytoplankton diversity in ocean biogeochemistry becomes widely recognized, the description of plankton in ocean ecological models is becoming more sophisticated. This means that a growing number of plankton physiological traits need to be determined for various species and under various growth conditions. We investigate how these traits can be estimated efficiently from common batch culture and chemostat experiments. We use the Metropolis algorithm, a random-walk Monte Carlo method, to estimate phytoplankton parameter values, along with the uncertainties in these values. First, we fit plankton physiological models to high-resolution batch culture and chemostat data sets to obtain parameter sets that are as accurate as possible. Then, we subsample these data sets and assess to which extent the accuracy is sacrificed when fewer measurements are taken. Two measurement points within the exponential growth stage of the batch culture data set are sufficient to constrain the maximum protein synthesis rate, the maximum photosynthesis rate, and the chlorophyll-to-nitrogen ratio. Two measurements during the stationary phase of the batch culture experiment are then enough to constrain the parameters related to carbon excretion and the photoacclimation time. From the chemostat experiment, only four measured points are needed to constrain the parameters connected with the internal reserve dynamics of phytoplankton. Thus, we demonstrate that traits related to key biogeochemical and physiological processes can be determined with only a few batch culture and chemostat measurements, as long as the measurement points are selected appropriately.

Phytoplankton blooms play a central role in the ocean carbon cycle, because much carbon export takes place during these events (Karl et al. 2003). During phytoplankton blooms, a wealth of different processes are occurring at the same time. A good example is provided by an observational study of a bloom in the Bedford Basin on the Nova Scotia coast (Kepkay et al. 1997). Chlorophyll, organic carbon, and organic nitrogen increase rapidly, while inorganic nutrients are depleted. Subsequently, chlorophyll, organic carbon, and organic nitrogen decrease again. During the bloom, the C : N ratio of the organic matter is higher than before or after the bloom. Understanding the dynamics of the C : N (and C : P) ratio in particular is crucial, because this stoichiometric ratio determines the strength of the soft-tissue carbon pump (Broecker 1982; Volk and Hoffert 1985; Omta et al.

2006). Batch and chemostat culture experiments can be used to mimic all these developments in the laboratory. More specifically, the exponential growth stage of a batch culture experiment is similar to the exponential growth stage of a phytoplankton bloom, as chlorophyll, organic carbon, and organic nitrogen increase rapidly, while inorganic nutrients are depleted. The stationary stage of a batch experiment then mimics the stage when the cells become nutrient-starved, followed by the subsequent demise of the bloom. A chemostat experiment reflects balanced growth conditions that may be representative of plankton in (tropical) regions without strong seasonal blooms.

A shift in algal stoichiometry due to nutrient depletion is evident in batch culture measurements presented in Fig. 1 (Flynn et al. 1994): as nitrogen becomes more limiting, the phytoplankton C : N ratio increases. Algal stoichiometric ratios can also shift due to changes in phytoplankton growth rate which can be studied under controlled conditions in a chemostat experiment. All these processes can be described

*Correspondence: omta@mit.edu

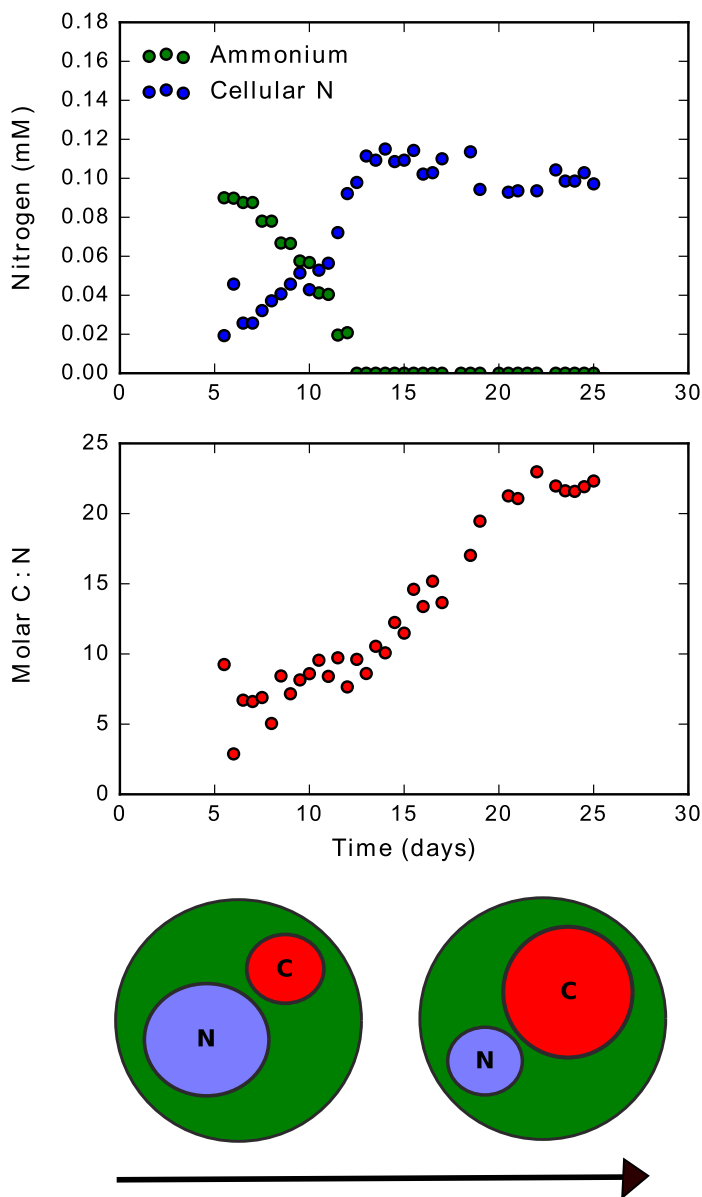Additional Supporting Information may be found in the online version of this article.

Fig. 1. Batch culture measurements for *Isochrysis galbana* of ammonium and cellular nitrogen (upper panel) and the organic C : N ratio (middle panel) from Flynn et al. (1994). As the inorganic nitrogen becomes depleted, the internal phytoplankton reserves shift from nitrogen toward carbon, a process schematically depicted in the lower panel.

by plankton physiological models. Combining the physiological models and the measurements, phytoplankton traits can be constrained. These traits can, in turn, be used in coupled ocean ecological models with which predictions can be made regarding the global carbon cycle (Vallina et al. 2014). Rates of photosynthesis, protein synthesis, and internal reserve turnover are key traits for describing plankton growth and C : N stoichiometry in ocean biogeochemical models (Omta et al. 2009; Arteaga et al. 2014). Another

important trait is the regulation of the cellular chlorophyll content, because chlorophyll is the one biogeochemical variable that is routinely observed at a high spatial and temporal resolution. Therefore, inclusion of chlorophyll (rather than simply biomass) is crucial, if ocean carbon cycle models are to be evaluated (Hemmings et al. 2008). Finally, carbon and nitrogen excretion are to be considered, because the associated microbial loop (Azam et al. 1994) may play an important role in regulating the export of organic carbon to the deep ocean (Anderson et al. 2007).

Laboratory experiments specifically targeted at each of these traits tend to be very labor-intensive. Plankton physiological traits may instead be estimated from oceanographic time series, as was done recently by Mutshinda et al. (unpubl.). Alternatively, these traits can be estimated by fitting plankton physiological models to more straightforward batch culture and chemostat measurements. However, even these relatively straightforward experiments are difficult to sample at high resolution. Accurately measuring the low biomass concentrations during the early exponential phase requires a very large sample volume. This is particularly problematic for small bacterioplankton such as *Prochlorococcus* and the SAR11 clade which are some of the most ubiquitous marine organisms (Partensky et al. 1999; Rappe et al. 2002). For example, Bertilsson et al. (2003) harvested and analyzed *Prochlorococcus* in a 75 mL culture at concentrations of about 10^8 cells/mL. To approach environmentally relevant concentrations of $1–3 \times 10^5$ cells/mL (Partensky et al. 1999), the culture would need to be diluted to at least 25 L. With chemostats, the long times needed to collect enough sample at low dilution rates are problematic. Thus, if environmentally relevant growth regimes are to be sampled, then it is crucial to minimize the number of measurements. It is not a priori clear how many measurements are needed to constrain plankton physiological models accurately, because these models generally consist of coupled nonlinear differential equations. To investigate to what extent the accuracy of the trait estimation is sacrificed when fewer measurements are taken, we first estimate traits by fitting results of plankton physiological models to experimental data of batch cultures (Flynn et al. 1994) and of a chemostat (Elrifi and Turpin 1985). What sets both these data sets apart from others is a combination of a high signal-to-noise ratio and an extraordinarily high resolution which means that the parameter estimates can be as accurate as possible. Then, we subsample the batch culture and chemostat data sets, perform the parameter estimates anew and compare the estimates from the full and reduced data sets. Although we limit ourselves to two data sets and two models here, we wish to emphasize the broader applicability of our work. Most of the parameters are present in some form in many phytoplankton models and our procedure for retrieving them is rather generic.

Models

The batch culture model (described in detail in "Batch culture" section) was modified from Geider et al. (1998). It describes the uptake of carbon and nitrogen and their conversion into phytoplankton biomass. With this model, we attempt to describe measurements of the growth of the haptophyte *Isochrysis galbana* in batch culture (Flynn et al. 1994). The chemostat model (described in detail in "Chemostat" section) follows ideas about the relationship between internal nutrient stores and the growth rate (Caperon and Meyer 1972; Droop 1973). These original models are the basis of our simpler models that resolve fewer processes and thus include less parameters. This is because with limited data, one can either constrain a small number of parameters well or a large number of parameters relatively poorly. For our purpose, it is crucial to have a benchmark of well-constrained parameters which means that the models need to be as simple as possible.

Batch culture

Our batch culture model has organic carbon (CH in units mM C), organic nitrogen contained in amino acids + proteins (PR in mM N) and chlorophyll (Chl in mM Chl) as variables, because these are the measured quantities in the Flynn et al. (1994) batch culture data set. The sources of CH and PR are determined by photosynthesis at a rate CH_{synth} (mol C/mol N d^{-1}) and protein synthesis at a rate PR_{synth} (d^{-1}). Both these rates are multiplied with the cell's PR content in the equations for the dynamics of CH and PR, because PR is assumed to be a measure of the amount of synthetic apparatus present in the phytoplankton. We assume that the photosynthesis rate CH_{synth} is constant throughout the experiment, neglecting the diurnal light : dark cycle, because the diurnal variations in CH and Chl are not very clear in the Flynn et al. (1994) measurements (Fig. 2). The organisms use carbon for protein synthesis at a rate $CN_{ratio} \times PR_{synth}$ (with CN_{ratio} the average C : N ratio of the amino acids in mol C/mol N); carbon is also lost through excretion (at a rate excr in d^{-1}). The cells acclimate by increasing their chlorophyll content when their carbon content is low and by decreasing their chlorophyll content when their carbon content is high. This is formulated mathematically through a target Chl : protein ratio θ_{tar} (nmol Chl/mmol N), toward which the Chl : protein ratio relaxes on a timescale τ which can be thought of as the inverse of Chl or photosystem biosynthesis/degradation rates. This target Chl : protein ratio increases linearly with increasing N : C ratio: $\theta_{tar} = b \times \left(\frac{PR}{CH}\right)$, with proportionality constant b (nmol Chl mmol C mmol N^{-2}).

Some other models also describe photoacclimation (partly) in terms of the C : N quota (Flynn and Flynn 1998; Ross and Geider 2009). These formulations are much more complicated than the target Chl : protein formulation; we chose our formulation for its simplicity. Phytoplankton mortality
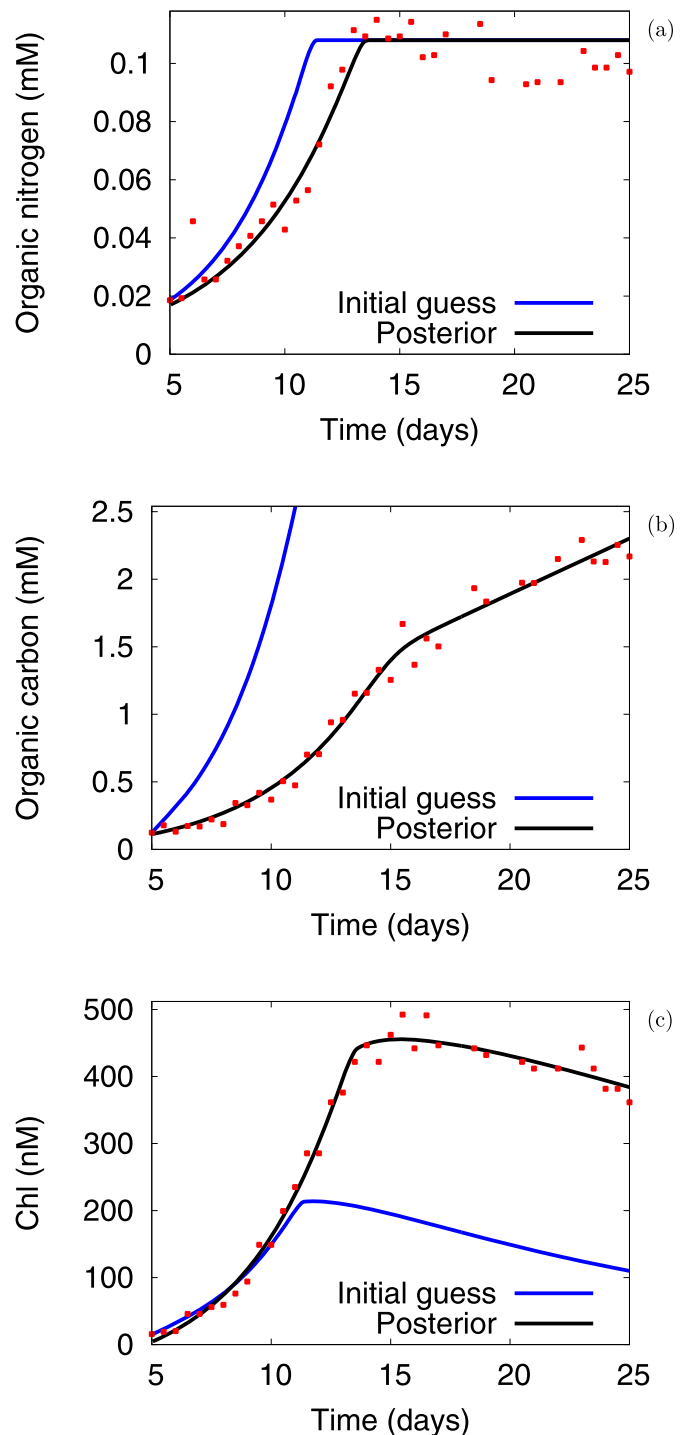

Fig. 2. Model-data comparison for (**a**) organic nitrogen (mM N), (**b**) organic carbon (mM C), and (**c**) chlorophyll (nM Chl). Blue lines represent model results for the initial-guess parameter set, black lines for posterior parameter set, red dots are data for *Isochrysis galbana* (Flynn et al. 1994).

is not included in our model; the decrease in particulate organic nitrogen during the stationary phase of the Flynn et al. (1994) batch experiment (Fig. 2a) seems too small to

constrain a mortality rate well. Thus, the dynamic equations become:

$$\frac{d\text{CH}}{dt} = \text{PR} \times \left(\text{CH}_{\text{synth}} - \text{CN}_{\text{ratio}} \times \text{PR}_{\text{synth}} - \text{excr}\right) \quad (1)$$

$$\frac{d\theta}{dt} = \frac{(\theta_{\text{tar}} - \theta)}{\tau} \quad (2)$$

$$\frac{d\text{PR}}{dt} = \text{PR} \times \text{PR}_{\text{synth}} \quad (3)$$

with $\theta = \frac{\text{Chl}}{\text{PR}}$ the chlorophyll to protein ratio at any given time. Protein synthesis is directly a function of the ambient inorganic nitrogen (N_{in} in mM N) concentration, according to Michaelis–Menten kinetics:

$$\text{PR}_{\text{synth}} = \frac{\mu_{\text{PR}} \times N_{\text{in}}}{\text{KN}_{\text{in}} + N_{\text{in}}} \quad (4)$$

with saturation constant KN_{in} and maximum protein synthesis rate μ_{PR}.

Under nitrogen limitation, the molar C : N ratio can become as high as 20–25 mol C/mol N. The following function of the cellular C : N ratio effectively forces the cell to excrete carbon at a rate excr when the C : N ratio of the cell (R_{cell} in mol C/mol N) is higher than a threshold value R_{exc} (mol C/mol N):

$$\text{excr} = \frac{m_{\text{exc}} \times \left(1 + \tanh\left(R_{\text{cell}} - R_{\text{exc}}\right)\right)}{2} \quad (5)$$

Chemostat

Our chemostat model distinguishes organic carbon, organic nitrogen, and organic phosphorus, as organic C : N : P ratios are the measured quantities in the Elrifi and Turpin (1985) chemostat data set. Furthermore, we make a distinction between nitrogen and phosphorus in functional biomass (N_F in mM N and P_F in mM P, connected through a constant N : P ratio R_{NP} in mol N/mol P, that is $N_F = P_F \times R_{\text{NP}}$) and nitrogen and phosphorus in reserve biomass (P_R in mM P and N_R in mM N). The uptake of carbon, nitrogen, and phosphorus is proportional to the functional biomass. With inflow concentrations N_i (mM N) and P_i (mM P) and dilution rate d (d^{-1}), we have the following dynamic equations for the inorganic nutrients nitrogen and phosphorus in the medium (N in mM N and P in mMP, respectively):

$$\frac{d\text{N}}{dt} = d \times (N_i - N) - N_{\text{upt}} \times N_F \quad (6)$$

$$\frac{d\text{P}}{dt} = d \times (P_i - P) - P_{\text{upt}} \times P_F \quad (7)$$

In principle, the nitrogen uptake rate could be chosen to follow Michaelis–Menten kinetics with the inclusion of a saturation constant. However, this saturation constant would have very little impact on the model predictions, because

nitrogen is not a limiting nutrient in the data set that we are fitting. Therefore, we simply take the nitrogen uptake rate N_{upt} (d^{-1}) equal to the maximum nitrogen uptake rate $V_{m,N}$ (d^{-1}):

$$N_{\text{upt}} = V_{m,N} \quad (8)$$

The uptake rate of the limiting nutrient phosphorus P_{upt} (mol P/mol N d^{-1}) follows Michaelis–Menten kinetics, with maximum uptake rate $V_{m,P}$ (mol P/mol N d^{-1}) and saturation constant KP (mM P):

$$P_{\text{upt}} = \frac{V_{m,P} \times P}{\text{KP} + P} \quad (9)$$

The nitrogen and phosphorus are assimilated into the nitrogen and phosphorus reserves N_R and P_R that are, in turn, mobilized for growth at a rate μ (d^{-1}). In general, the growth rate depends critically on the reserve concentration (or quota) of the limiting nutrient inside the organisms (Droop 1973; Kooijman 2010) which is in this case phosphorus. We describe the transfer of reserve to functional biomass with Michaelis–Menten kinetics, because this transformation represents a complex of enzymatic reactions:

$$\mu = \frac{V_{m,QP} \times \chi_P}{\text{KQP} + \chi_P} \quad (10)$$

with $\chi_P = \frac{P_R}{P_F}$; $V_{m,QP}$ (d^{-1}) is the maximum functional biomass synthesis rate and KQP is a dimensionless saturation constant.

The dynamics of the nitrogen reserve N_R is driven by uptake, excretion (at a rate excr_N in d^{-1}), mobilization for growth, and dilution:

$$\frac{d\text{N}_R}{dt} = N_{\text{upt}} \times N_F - \text{excr}_N \times N_R - \mu \times N_F - d \times N_R \quad (11)$$

while the functional biomass is simply governed by growth and dilution:

$$\frac{d\text{N}_F}{dt} = (\mu - d) \times N_F \quad (12)$$

$$\frac{d\text{P}_F}{dt} = (\mu - d) \times P_F \quad (13)$$

Carbon is taken up and excreted at rates P_m (mol C/(mol N d)) and excr_C (d^{-1}), leading to the following equation for organic carbon C_R (mM C):

$$\frac{d\text{C}_R}{dt} = P_m \times N_F - \text{excr}_C \times C_R - d \times C_R \quad (14)$$

In Web Appendix A, the steady-state solutions of these equations are derived. These solutions give rise to complete expressions for the algal stoichiometric ratios (A.3 and A.5), which are then fitted against the chemostat data.

Table 1. Variables and parameter values for the batch culture model with associated units.

Symbol	Description	Initial guess	Posterior value	Units
CH	Carbohydrate/lipid			mM C
PR	N in protein			mM N
Chl	N in chlorophyll *a*			nM Chl
R_{cell}	C:N ratio of the cell			mol C/mol N
CN_{ratio}	C:N of protein	6.6		mol C/mol N
KN_{in}	Half-sat. N	0.002		mM N
μ_{PR}	Max. prot. synth. rate	0.3	0.234 ± 0.002	d^{-1}
CH_{synth}	Max. photosynth. rate	10	2.19 ± 0.02	mol C/(mol N d)
m_{exc}	Max. C excr. Rate	2.0	1.43 ± 0.02	mol C/(mol N d)
R_{exc}	C:N ratio above which excr. happens	10.0	13.49 ± 0.11	mol C/(mol N)
τ	Photoacclimation time	1.0	9.59 ± 0.13	days
b	Chl:N target increase per amount of change in N:C ratio	1	57.1 ± 0.2	(nmol Chl mmol Cmmol N^{-2})
CH_{ini}	Initial carb. conc.	0.1242	0.112 ± 0.003	mM C
PR_{ini}	Initial prot. conc.	0.0186	0.0169 ± 0.0002	mM N
Chl_{ini}	Initial Chl conc.	15	41 ± 10	nM Chl

Simulations and trait estimation

To investigate how phytoplankton traits can be estimated from observations in an efficient manner, we use the following procedure. For the two models formulated in the previous section, we first estimate parameter sets that are as accurate as possible using high-resolution measurements of the haptophyte *Isochrysis galbana* in batch culture (Flynn et al. 1994) and of the chlorophyte *Selenastrum minutum* in continuous culture (Elrifi and Turpin 1985). Subsequently, we reduce the number of points in each data set and quantify the loss of accuracy. Furthermore, we vary the distance between the measured points to investigate the impact on the accuracy of the parameters. In this way, we aim to inform experimentalists which measurements to take for an effective determination of phytoplankton traits. We use the Metropolis algorithm described in Web Appendix B; the source code has been included as online Supporting Information Material.

Parameter estimation: batch culture

We start from an initial guess for the parameters (listed in Table 1) estimated through visual trial-and-error optimization. For these parameters, the model agrees well with the measured organic nitrogen, but not with the measured organic carbon and chlorophyll (Fig. 2, blue lines). The data from the first 5 d of the batch culture experiment are discarded, as in Geider et al. (1998), because the organisms have not yet reached their maximum growth rate during this initial lag phase. In total, we estimate nine parameters: six physiological traits (μ_{PR}, CH_{synth}, m_{exc}, R_{exc}, b, τ), as well as the initial concentrations of chlorophyll, organic carbon, and organic nitrogen. The half-saturation constant for amino acid synthesis KN_{in} is kept fixed, because this parameter

Table 2. Correlations (r^2) between fitting parameters of the batch culture model.

	μ_{PR}	CH_{synth}	m_{exc}	b	R_{exc}	τ
μ_{PR} (d^{-1})	1	0.13	0.09	0.007	0.07	0.04
CH_{synth} (mol C/mol N d^{-1})	0.13	1	0.76	0.003	0.41	0.05
m_{exc} (mol C/mol N d^{-1})	0.09	0.76	1	0.0008	0.05	0.03
b (nmol Chl mmol Cmmol N^{-2})	0.007	0.003	0.0008	1	0.03	0.05
R_{exc} (mol C/mol N)	0.07	0.41	0.05	0.03	1	0.08
τ (d^{-1})	0.04	0.05	0.03	0.05	0.08	1

could not be constrained well using the Flynn et al. (1994) data set. For the Metropolis procedure, measurement uncertainties are needed, which Flynn et al. (1994) did not provide. Based on a visual estimate of the spreads in the measured values (in particular during the stationary phase), these uncertainties are taken equal to 2 μM, 10 μM, and 2 nM for the organic nitrogen, organic carbon and chlorophyll concentrations, respectively. The results of a simulation using the posterior mean parameter values are shown as the black lines in Fig. 2: both the organic carbon and chlorophyll show tremendous improvement compared with the initial-guess parameter set. There is some correlation between the parameters (Table 2), in particular between the
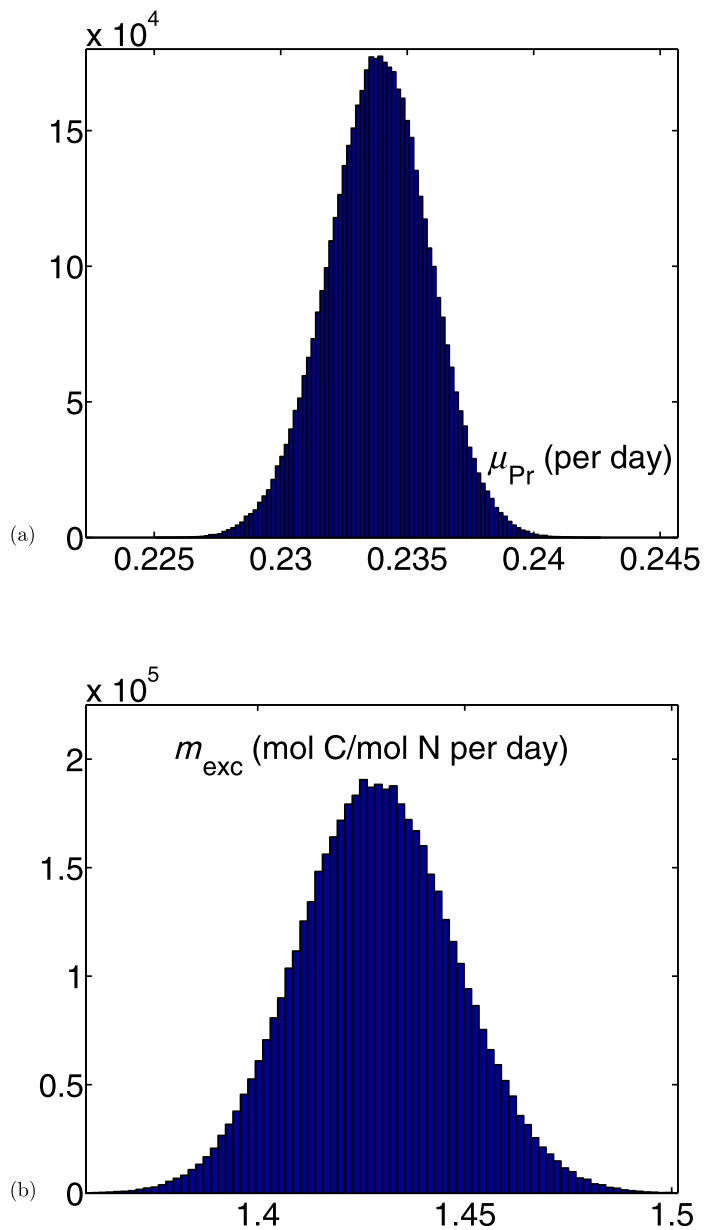
Fig. 3. Posterior parameter distributions: μ_{PR} (**a**), m_{exc} (**b**). For easy comparison of the distribution relative to each other, each figure covers a factor 0.1 of the respective parameter. To prevent distortion due to autocorrelation, every 10th sample has been used for plotting the distributions.

photosynthesis rate (P_m) and the carbon excretion rate (m_{exc}). Essentially, this reflects that a high estimate of the photosynthesis rate can be compensated to some extent by a high estimate of the carbon excretion.

Some of the posterior parameter values can be compared with independent measurements. For example, radiocarbon measurements indicate a photosynthesis rate of about 1.5 d^{-1} for *Isochrysis galbana* during the exponential growth stage (Hobson et al. 1979). This corresponds to about 10 mol
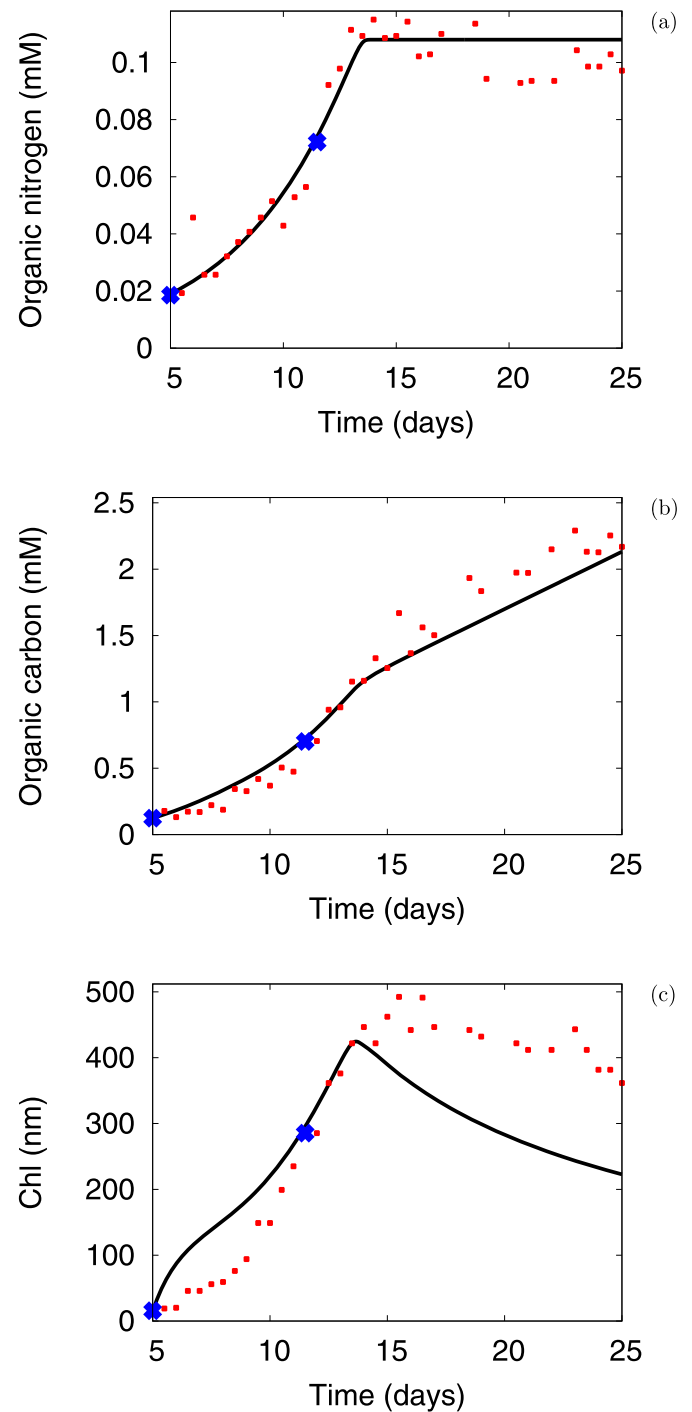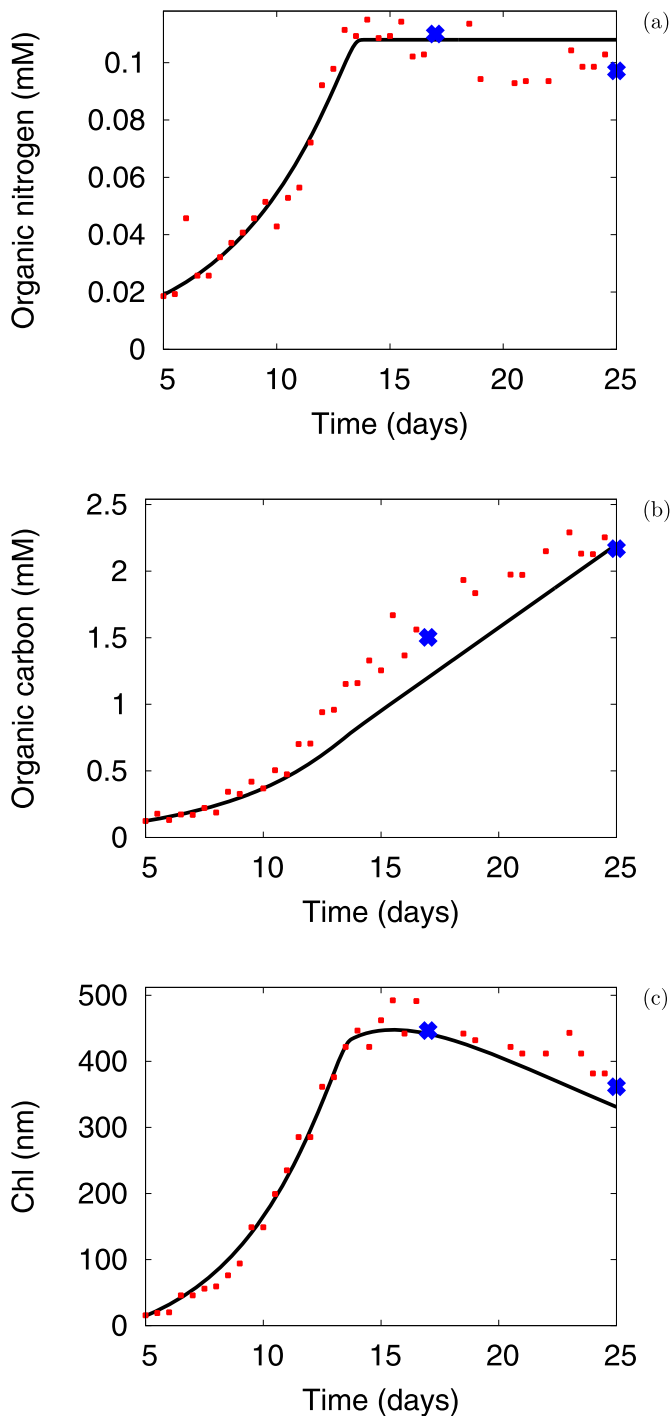

Fig. 4. Model-data comparison for posterior parameter set with a reduced batch culture data set. Black lines are the model predictions using the parameters estimated only from the two blue data points in the exponential phase, for (**a**) organic nitrogen (mM N), (**b**) organic carbon (mM C), and (**c**) chlorophyll content (nM Chl). The data points that were not used in this parameter estimate are in red.

C/mol N d^{-1}, much higher than the 2.19 ± 0.02 mol C/mol N d^{-1} determined here. Possibly, our estimated P_m does not correspond with the true maximum photosynthesis rate,

Fig. 5. Model-data comparison for posterior parameter set with a reduced batch culture data set. Black lines are the model predictions using the parameters estimated only from the two blue data points in the stationary phase, for (**a**) organic nitrogen (mM N), (**b**) organic carbon (mM C), and (**c**) chlorophyll content (nM Chl). The data points that were not used in this parameter estimate are in red.

Fig. 6. For the stationary phase, the precision and the accuracy of the estimated parameters τ (green) and m_{erc} (red) depend on both the number of data points used and the distance between those data points. In panel (**a**), the distance between the points is kept fixed at 2 d and the number of points is varied. In panel (**b**), the number of points is kept fixed at 2, while the distance between the points is varied. In each case, $t = 17$ d is used as the first fitting data point. Vertical axes: ratio of parameter values obtained from the limited data set to parameter values from the full data set.

because the 20 W/m^2 irradiation used by Flynn et al. (1994) may not have been sufficient to saturate the algae completely. Moreover, Flynn et al. (1994) included a diurnal light : dark cycle in their experiment. Thus, we are in fact considering an average photosynthesis rate under a diurnal light : dark cycle. The photoacclimation time may be compared to measurements of the turnover of radiolabeled chlorophyll. We are not aware of such measurements for *Isochrysis galbana*; for the diatom *Skeletonema costatum*, values between 3 h and 9 h were measured (Riper et al. 1979), which is an order of magnitude faster than our parameter estimate $\tau = 9.59 \pm 0.13$ d. This difference probably reflects the very fast growth rate of *S. costatum*, with division rates up to 2 d^{-1} (Hitchcock 1980) which is also an order of

Table 3. Parameter estimates for the batch culture model with associated units when using 7 data points.

Symbol	Description	Initial guess	Posterior value	Units
μ_{PR}	Max. prot. synth. rate	0.3	0.292 ± 0.007	d^{-1}
CH_{synth}	Max. photosynth. rate	10	2.36 ± 0.09	mol C/(mol N d)
m_{exc}	Max. C excr. rate	2.0	1.50 ± 0.09	mol C/(mol N d)
R_{exc}	C : N ratio above which excr. happens	10.0	11.5 ± 0.2	mol C/(mol N)
τ	Photoacclimation time	1.0	9.2 ± 0.3	days
b	Chl : N target increase per amount of change in N : C ratio	1	57.6 ± 0.3	(nmol Chl mmol Cmmol N^{-2})
CH_{ini}	Initial carb. conc.	0.1242	0.145 ± 0.007	mM C
PR_{ini}	Initial prot. conc.	0.0186	0.0130 ± 0.0006	mM N
Chl_{ini}	Initial Chl conc.	15	9.8 ± 1.6	nM Chl

magnitude faster than *I. galbana*. Most of the other parameter values obtained here cannot be compared directly with parameter values from other studies because of differences in the model formulation. For example, the original Geider et al. (1998) model included nitrogen quota (internal storage in, e.g., vacuoles), in contrast with our batch culture model. Remarkably, we are able to fit the organic carbon data well during both the exponential phase and the stationary phase, whereas Geider et al. (1998) were able to fit only the exponential phase well. Probably, our improved fit is due to the search algorithm that formally minimizes a cost function. In Fig. 3, histograms of the posterior values are shown for some of the parameters. The posterior distribution of the maximum protein synthesis rate (μ_{PR}) is relatively narrow, with $\frac{\sigma}{\mu}$ =0.015, in comparison to the posterior distribution of the carbon excretion rate (m_{exc}), with $\frac{\sigma}{\mu}$ =0.028, which suggests that the mean estimate of μ_{PR} is less uncertain than the mean estimate of m_{exc}.

Reducing the number of measured points from the batch culture data set, we take careful consideration of the fact that the exponential growth phase provides insight into maximum rates, whereas the stationary phase can give information about carbon excretion under nutrient stress. Since an exponential curve is completely determined by two points, we optimize the maximum protein synthesis rate (μ_{PR}), the maximum photosynthetic rate (CH_{synth}) and the photoacclimation parameter (b) using only the measurements at 5 d and 11.5 d after the beginning of the Flynn et al. (1994) experiment. Starting with the same initial-guess parameter values as in the fit with the full data set, we obtain $\mu_{PR} = 0.217 \pm 0.018$ d^{-1}, $P_m = 2.8 \pm 0.3$ mol C/mol N d^{-1}, $b = 39 \pm 2$ nmol Chl mmol C mmol N^{-2} (fits shown in Fig. 4). Notably, the parameters have posterior values rather close (0–30% difference) to the ones obtained from fitting the full data set.

While the population does not grow anymore during the stationary phase, the organisms still perform photosynthesis, which leads to an accumulation of excess carbohydrate in the cells. Once their C : N ratio exceeds a certain threshold, the cells may start to excrete part of the excess carbohydrate (Zlotnik and Dubinsky 1989; Myklestad 1995). We found that the photoacclimation time (τ), the maximum rate of carbon excretion (m_{exc}) and, to some extent, the threshold C : N ratio above which carbon excretion occurs (R_{exc}) can be constrained using data from the stationary phase alone. In Fig. 5, we show a fit using two stationary phase measurement points (at 17 d and 21 d). The parameter values obtained through this fit are $\tau = 7.22 \pm 0.12$ d and $m_{exc} = 1.341 \pm 0.005$ mol C/mol N d^{-1} which are on average about 15% different from the values obtained through the fit against the full data set; R_{exc} was unconstrained by this fit. How close the fitted values are to the values estimated from the entire data set depends strongly on the number of data points used for the fit, as well as on the distance between those data points. This is illustrated in Fig. 6 where we plot the ratio of the parameter values obtained from the reduced data set to the parameter values from the full data set. We think that this is a very informative measure: for example, one can immediately see that with 2 points at a distance of 2 d, τ is underestimated by 40%. With 5 data points separated by 2 d, τ and m_{exc} are within 10% of the values estimated from the full data set. We need 7 data points (three in the exponential phase, four in the stationary phase) to estimate all parameters accurately (parameter estimates in Table 3, fits in Fig. 7).

Parameter estimation: chemostat

First, we rearrange the model equations as described in Web Appendix A to enable straightforward calculations for the millions of iterations of the Metropolis procedure. That is, we set all the time derivatives equal to 0, because the chemostat is at steady state when each of the measurements is taken. Then, the system is reformulated into equations for the algal stoichiometric ratios (A.3 and A.5). Starting the parameter optimization procedure, we perform a simulation with the initial-guess parameter set listed in Table 4; the
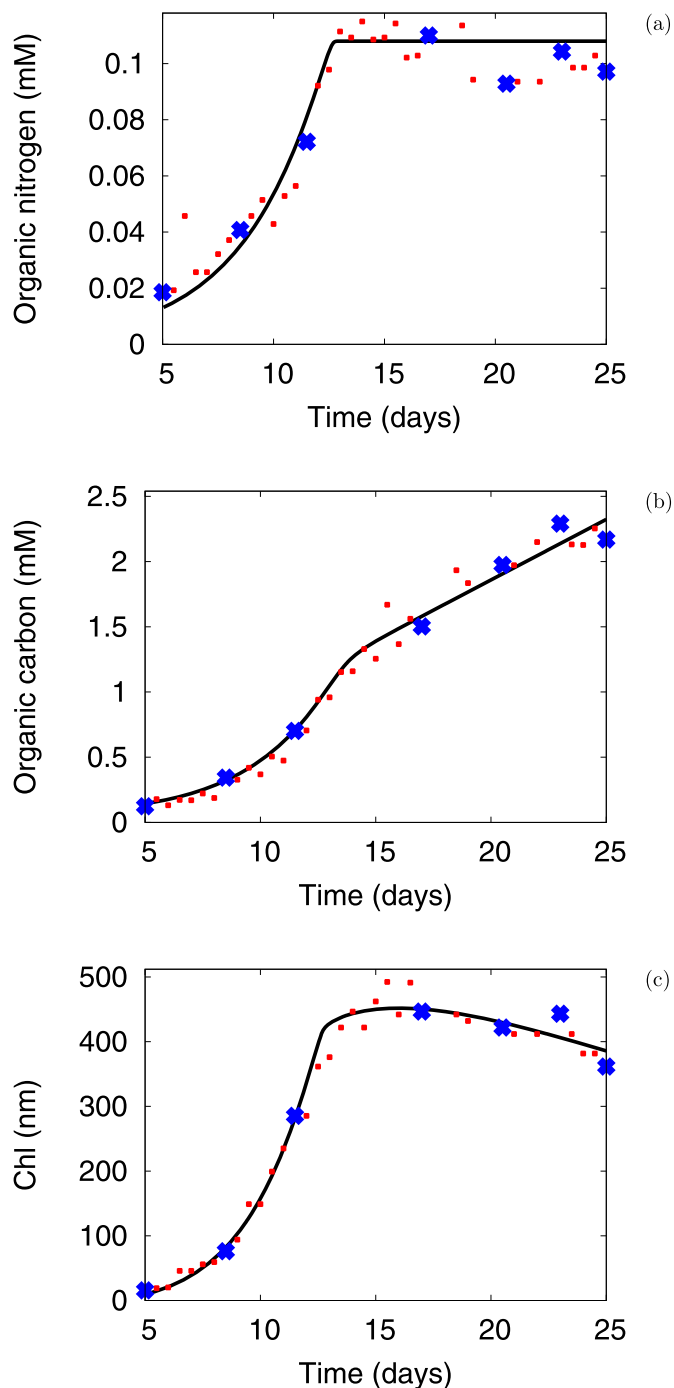
Fig. 7. Model-data comparison for posterior parameter set with a reduced batch culture data set. Black lines are the model predictions using the parameters estimated only from the seven blue data, for (**a**) organic nitrogen (mM N), (**b**) organic carbon (mM C), and (**c**) chlorophyll content (nM Chl). The data points that were not used in this parameter estimate are in red.

Table 4. Variables and parameter values for the chemostat model with associated units.

Symbol	Description	Initial guess	Posterior value	Units
N	Inorg. nitr.			mM N
P	Inorg. phosph.			mM P
N_F	N in funct. biomass			mM N
N_R	N in reserve biomass			mM N
P_F	P in funct. biomass			mM P
P_R	P in reserve biomass			mM P
C_R	C in biomass			mM C
d	Dilution rate			d^{-1}
N_i	Input N	2000		μM N
P_i	Input P	10		μM P
KP	Half-sat. P uptake	0.0001		μM P
KQP	Half-sat. funct. biomass synthesis	0.8		——
R_{NP}	Redfield N : P	16		mol N/mol P
$V_{m,N}$	Max. N uptake rate	5.0	4.25 ± 0.13	d^{-1}
$V_{m,P}$	Max. P uptake rate	5.0		mol P/(mol N d)
$V_{m,QP}$	Max. funct. biomass synthesis rate	2.5	2.7 ± 0.3	d^{-1}
P_m	Photosynthesis rate	10.0	22.2 ± 1.1	mol C/(mol N d)
$excr_C$	C loss rate	0.4	0.37 ± 0.03	d^{-1}
$excr_N$	N loss rate	1.0		d^{-1}

and the carbon excretion $excr_C$) against chemostat measurements of the chlorophyte *Selenastrum minutum* under phosphorus limitation (Elrifi and Turpin 1985). We use measurement uncertainties of 0.6 mol C/mol N, 40 mol C/mol P, and 5 mol N/mol P for the C : N, C : P, and N : P ratios, respectively, again based on a visual estimate, because Elrifi and Turpin (1985) did not provide standard errors. The half-saturation constants for phosphorus uptake and functional biomass synthesis (KP and KQP, respectively), as well as the maximum phosphorus uptake rate $V_{m,P}$ and the nitrogen excretion $excr_N$ are kept constant, because these parameters cannot be constrained well using the chemostat measurements. The results of a simulation using the posterior mean parameter values ($P_m = 22.2 \pm 1.1$ mol C/mol N d^{-1}, $V_{m,N} = 4.25 \pm 0.13$ d^{-1}, $V_{m,QP} = 2.7 \pm 0.3$ d^{-1}, $excr_C = 0.37 \pm 0.03$ d^{-1}) are shown as the black lines in Fig. 8. There is some correlation between the parameters, in particular between the photosynthesis rate P_m and the carbon excretion rate $excr_C$ (Table 5). Again, this reflects that a high estimate of the photosynthesis rate can be compensated to some extent by a high estimate of the carbon excretion. Nevertheless, even these parameters are constrained within 5–10% of their mean posterior values. An ammonium pulse
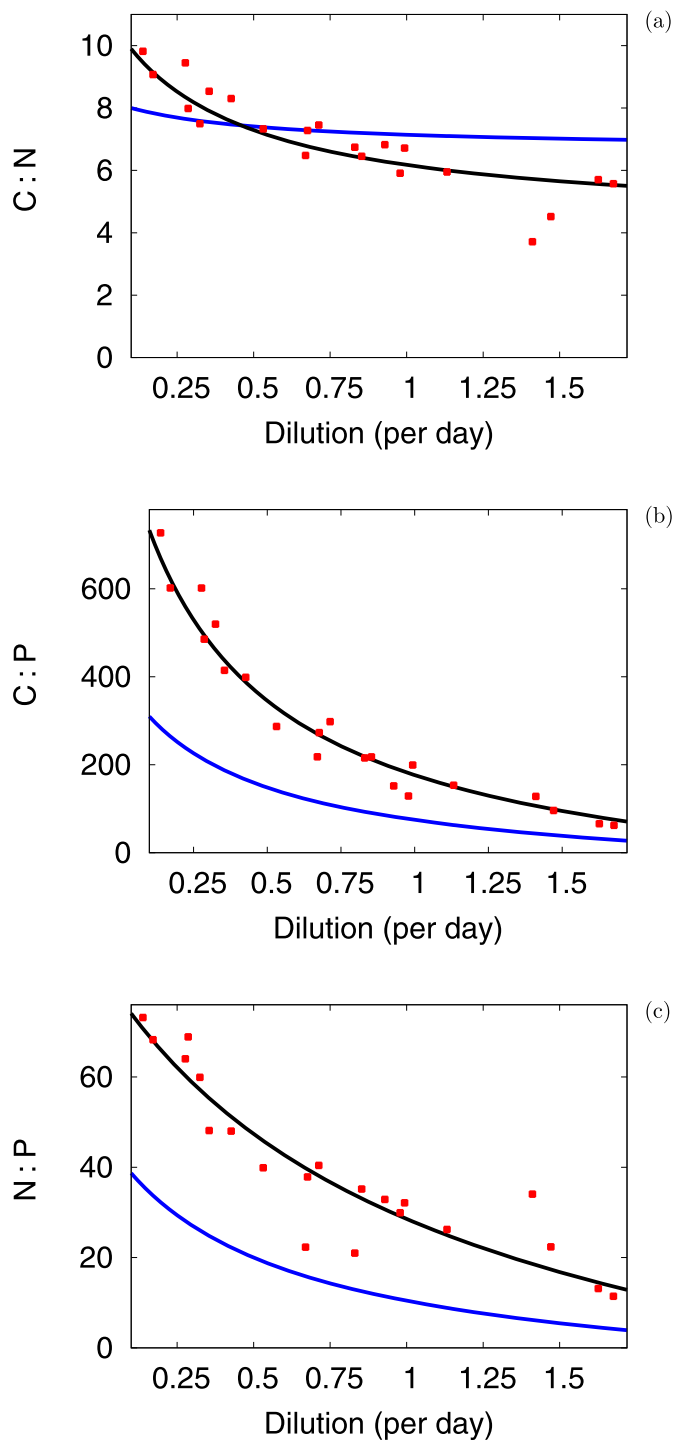
results are the blue lines in Fig. 8. We estimate four model parameters (the photosynthesis rate P_m, the nitrogen uptake rate $V_{m,N}$, the maximum reserve mobilization rate $V_{m,QP}$,

Fig. 8. Model-data comparison for initial-guess (blue lines) and posterior (black lines) parameter set of the chemostat model, with the red dots *Selenastrum minutum* measurements (Elrifi and Turpin 1985): (**a**) C : N ratio (mol C/mol N), (**b**) C : P ratio (mol C/mol P), (**c**) N : P ratio (mol N/mol P).

experiment gave a nitrogen assimilation rate of about 20 d^{-1} (Weger et al. 1988), much higher than our estimated $V_{m,N} = 4.25$ d^{-1}. Possibly, this difference is due to differences

Table 5. Correlations (r^2) between fitting parameters of the chemostat model.

	$V_{m,n}$	$V_{m,QP}$	P_m	$excr_C$
$V_{m,n}$ (d^{-1})	1	0.41	0.39	0.12
$V_{m,QP}$ (d^{-1})	0.41	1	0.26	0.09
P_m ($_{mol}$ C/$_{mol}$ N d^{-1})	0.39	0.26	1	0.80
$excr_C$ (d^{-1})	0.12	0.09	0.80	1

in the experimental setups. The organisms in the pulse experiment may be hoarding nitrogen temporarily as luxury uptake, whereas the population in the chemostat is at steady state.

When reducing the number of data points to 4, we obtain the following parameter values:

$P_m = 23 \pm 2$ mol C/mol N d^{-1}, $V_{m,N} = 4.4 \pm 0.3$ d^{-1},

$V_{m,QP} = 2.6 \pm 0.7$ d^{-1}, $excr_C = 0.35 \pm 0.05$ d^{-1} (fits in Fig. 9) which are on average 8% different from the values obtained using the full data set. Thus, four data points with a distance of about 0.5 d^{-1} between them appear sufficient to constrain the key parameters with a reasonable accuracy. Having at least one data point at a dilution rate close to the washout is very helpful, because the curvature of the stoichiometric ratios as a function of the dilution rate can be determined much better. And this curvature is what constrains the internal quota dynamics. If the highest measured dilution rate is 1.1 d^{-1} (instead of 1.7 d^{-1}), then the parameters can still be constrained accurately, but 10 data points with a distance of about 0.1 d^{-1} between them are needed. Hence, one either needs to perform at least one measurement in the difficult high-dilution range or one needs to perform a large number of measurements outside that range.

Discussion

Photosynthesis, nutrient uptake, and carbohydrate excretion are fundamental processes that link across many scales, being central elements of phytoplankton physiology, as well as ocean carbon biogeochemistry. As it has become clear that the rates of these processes are by no means constant, it has become imperative to determine how they depend on environmental conditions and how they vary among and within phytoplankton species. It is crucial to find an efficient way to carry this out, because determining growth parameters for a large number of species and under a large number of different conditions is very labor-intensive. Therefore, we have investigated the extent to which measurement effort can be reduced, while still obtaining accurate parameter estimates. To obtain
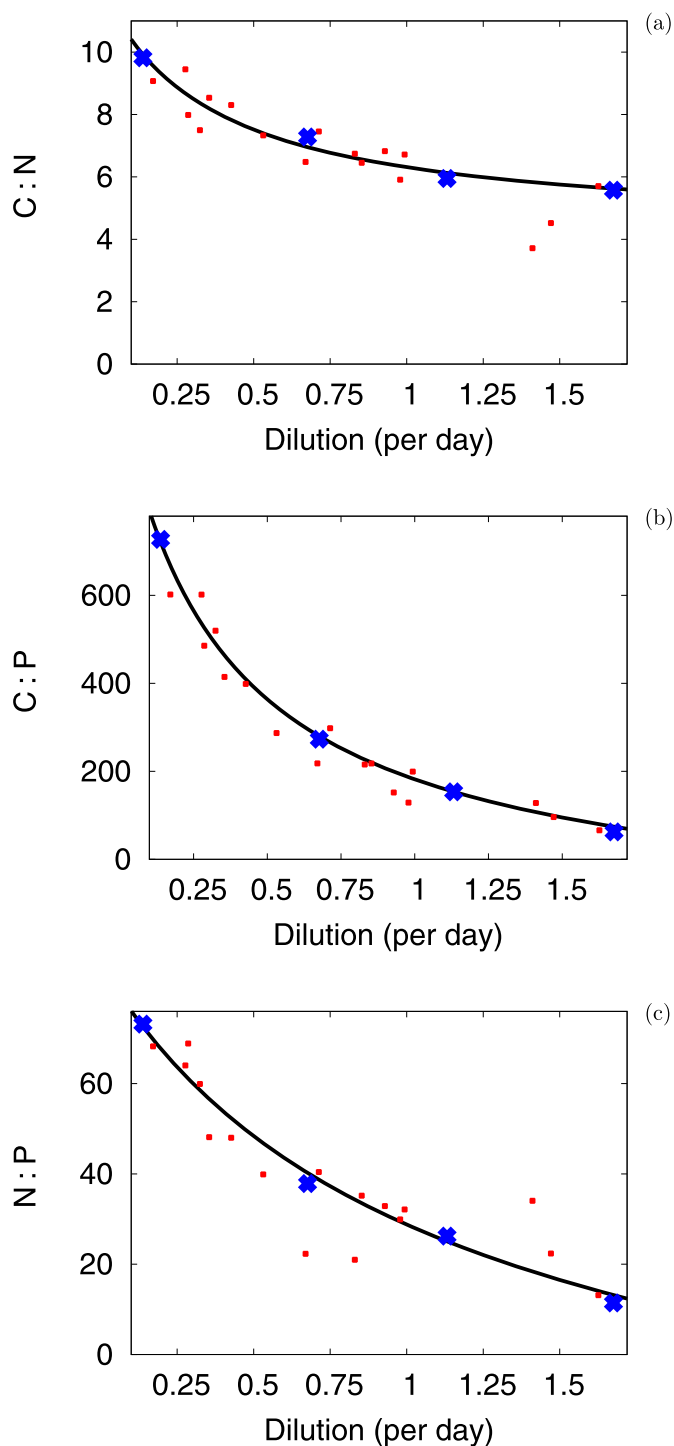
Fig. 9. Model-data comparison for posterior parameter set of the chemostat model using a reduced data set. Black lines are the model predictions using only the four blue data points: (**a**) C : N ratio (mol C/mol N), (**b**) C : P ratio (mol C/mol P), (**c**) N : P ratio (mol N/mol P). The data points that were not used in this parameter estimate are in red.

benchmark parameter estimates, we have first performed fits on full high-resolution data sets. Subsequently, we have subsampled these same data sets so that any differences in the

parameter values could be attributed to the lower resolution. In the future, this subsampling approach could be extended to different models and data sets than the ones we used. In that way, the variability in the traits between different species may be assessed. Fits by Flynn et al. (2008) indicate particularly strong variations in the release of dissolved organic matter.

Our results suggest that various key plankton physiological traits can be estimated well using relatively few measurements from common batch culture and chemostat experiments for the model equations imposed. Four data points from a chemostat experiment were needed to constrain the carbon excretion rate (which could alternatively be interpreted as photosynthesis downregulation), the maximum average photosynthesis rate under a diurnal light : dark cycle, the maximum nitrogen uptake rate, and the maximum internal phosphorus turnover rate. Two data points from the exponential phase of the batch culture experiment provided constraints on traits related to growth (maximum protein synthesis rate, maximum photosynthetic rate, Chl synthesis), whereas the carbon excretion rate and the photoacclimation time were estimated from two stationary phase data points. Thus, when attempting to constrain phytoplankton physiological parameters through a minimum number of batch culture measurements, it is crucial to monitor when the system transitions from the exponential to the stationary growth stage (using flow cytometry, microscopy or, if applicable, measurements of optical density or culture fluorescence). All this is predicated on having measurements with a sufficiently high signal-to-noise ratio. Our main findings do not apply, if the variance in the measurements is so high that it drowns out the key dynamics.

The traits estimated from the exponential phase of the batch culture experiment have a straightforward interpretation, since the rapid increases in organic nitrogen, organic carbon, and chlorophyll are driven by protein synthesis, photosynthesis, and chlorophyll synthesis, respectively. The interpretation of the slowdown in carbon accumulation during the stationary phase is somewhat less straightforward. In fact, Geider et al. (1998) interpreted it as a downregulation of photosynthesis, rather than excretion. Although much evidence has been compiled of organic matter excretion by phytoplankton through various processes (Thornton 2014), measurements of dissolved organic compounds would be needed to distinguish between carbon exudation and photosynthesis downregulation. The relatively small Chl decrease during the stationary phase of the Flynn et al. (1994) experiment (Fig. 2c) may indicate only a weak photosynthesis downregulation. However, it needs to be noted that Chl is only one component of the photosynthetic machinery. For example, the D1 protein could be damaged, leading to decreased photosynthesis, even if the Chl concentration remains high.

The traits estimated from the chemostat experiment all have rather indirect relationships with the actual

measurements. Nevertheless, algal stoichiometric ratios ultimately need to be connected with the uptake and release of C, N, and P, so a fundamentally different interpretation than the one underlying our chemostat model is difficult to envision. More direct measurements have given a similar value for the maximum photosynthesis rate, but a much higher value for the maximum nitrogen uptake rate which may be due to the specific setup of the experiment (see "Parameter estimation: chemostat" section). The carbon excretion rate $excr_C = 0.37$ d^{-1} estimated from the *Selenastrum minutum* chemostat data appears relatively low, also in comparison with our estimate from the *Isochrysis galbana* batch culture data. Another remarkable feature is that nitrogen excretion needed to be included for an optimal model fit. Indeed, recent work suggests that microorganisms excrete significant amounts of nitrogen (Suratman et al. 2008; Romera-Castillo et al. 2010; Mooshammer et al. 2014), although carbon excretion has received more attention in the past.

Some important traits could not be constrained well from the data that we used. For example, we attempted to estimate the half-saturation constant for protein synthesis (KN_{in}) from the batch culture data, but the Metropolis algorithm tended to push the value to 0. This does not mean that KN_{in} is really equal to 0, but rather that this parameter cannot be estimated from the batch culture measurements. To estimate KN_{in} accurately, the phytoplankton growth rate would have to be measured at different inorganic nitrogen concentrations as the culture shifts from nutrient-replete to nutrient-starved. In the Flynn et al. (1994) data set, there are simply too few data points within this transition. Generally, half-saturation constants are most effectively determined through targeted experiments, for example using radiolabeled nutrients (Button 1994). Although we were able to estimate photoacclimation parameters, the Flynn et al. (1994) experiment is actually, in our view, not optimally suited to constrain photoacclimation, because there are no clear diurnal variations in the Chl content. Other data sets with larger diurnal variations in Chl, for example Ross and Geider (2009), are likely helpful to constrain photoacclimation more precisely. Finally, we note that, in some cases, there exist multiple parameter combinations similar in their ability to produce good model-data fits, yet with different trait values (Löptien and Dietze 2015; Grossowicz et al. in press). In such a case, one expects bimodal or even trimodal parameter distributions, rather than the Gaussian distributions we found (Fig. 3).

Conclusion

To constrain the multi-dimensional trait space of phytoplankton, growth parameters need to be determined for a large number of species and under a large number of different conditions. This is very labor-intensive, which makes finding methods to limit the number of measurements imperative. We have demonstrated that key phytoplankton physiological traits can be extracted from a batch culture experiment with only four measurements. From a chemostat experiment, four data points were needed to extract the key traits. Any data set is rather specific, for example in terms of the species used and the measured quantities. This means that parameter values and even model formulations that we use are rather specific as well. Nevertheless, we think that our findings are rather general, because they can be understood from common mathematical features. Both exponential and linear functions are completely determined by two points. Therefore, two data points during each growth phase of a batch culture experiment are needed to constrain the various accumulation rates in the exponential and stationary growth phases. During the exponential phase, the rates are probably close to maximal, so they can be identified with the maximum protein synthesis, chlorophyll synthesis, and photosynthesis rates (under a diurnal light : dark cycle). From the difference in the carbohydrate accumulation rate between the stationary and exponential phases, a downregulation of photosynthesis or an enhanced carbon excretion can then be inferred. To constrain the hyperbolic internal quota dynamics from a chemostat experiment (in particular, the maximum functional biomass synthesis rate $V_{m,QP}$), four data points are needed, because the curvature in the measured stoichiometric ratios needs to be resolved well. Although actual parameter values will be different for each specific organism, our study shows which information is, in general, needed to extract these parameter values.

References

Anderson, T. R., A. Ryabchenko, M. J. R. Fasham, and V. A. Gorchakov. 2007. Denitrification in the Arabian Sea: A 3D ecosystem modelling study. Deep-Sea Res. I **54**: 2082–2119. doi:10.1016/j.dsr.2007.09.005

Arteaga, L., M. Pahlow, and A. Oschlies. 2014. Global patterns of phytoplankton nutrient and light colimitation inferred from an optimality-based model. Global Biogeochem. Cycles **28**: 648–661. doi:10.1002/2013GB004668

Azam, F., D. C. Smith, G. F. Stewart, and A. Hagstrom. 1994. Bacteria-organic matter coupling and its significance for oceanic carbon cycling. Microb. Ecol. **28**: 167–179. doi:10.1007/BF00166806

Bertilsson, S., O. Berglund, D. M. Karl, and S. W. Chisholm. 2003. Elemental composition of marine *Prochlorococcus* and *Synechococcus*: Implications for the ecological stoichiometry of the sea. Limnol. Oceanogr. **48**: 1721–1731. doi:10.4319/lo.2003.48.5.1721

Broecker, W. S. 1982. Ocean chemistry during glacial time. Geochim. Cosmochim. Acta **46**: 1689–1705. doi:10.1016/0016-7037(82)90110-7

Button, D. K. 1994. The physical base of marine bacterial ecology. Microb. Ecol. **28**: 273–285. doi:10.1007/BF00166817

Caperon, J., and J. Meyer. 1972. Nitrogen-limited growth of marine phytoplankton – Changes in population characteristics with steady-state growth rate. Deep-Sea Res. **19**: 601–618. doi:10.1016/0011-7471(72)90089-7

Dowd, M. 2005. A sequential Monte Carlo approach for marine ecological prediction. Environmetrics **17**: 435–455. doi:10.1002/env.780

Droop, M. R. 1973. Some thoughts on nutrient limitation in algae. J. Phycol. **9**: 264–272. doi:10.1111/j.1529-8817.1973.tb04092.x

Elrifi, I. R., and D. H. Turpin. 1985. Steady-state luxury consumption and the concept of optimum nutient ratios: A study with phosphate and nitrate limited *Selenastrum minutum* (Chlorophyta). J. Phycol. **21**: 592–602. doi:10.1111/j.0022-3646.1985.00592.x

Flynn, K. J., K. Davidson, and J. W. Leftley. 1994. Carbon-nitrogen relations at whole-cell and free-amino-acid levels during batch growth of *Isochrysis galbana* (Prymnesiophyceae) under conditions of alternating light and dark. Mar. Biol. **118**: 229–237. doi:10.1007/BF00349789

Flynn, K. J., and K. Flynn. 1998. The release of nitrite by marine dinoflagellates-development of a mathematical solution. Mar. Biol. **130**: 455–470. doi:10.1007/s002270050266

Flynn, K. J., R. Clark, and Y. Xue. 2008. Modeling the release of dissolved organic matter by phytoplankton. J. Phycol. **44**: 1171–1187. doi:10.1111/j.1529-8817.2008.00562.x

Geider, R. J., J. MacIntyre, and T. M. Kana. 1998. A dynamic regulatory model of phytoplanktonic acclimation to light, nutrients and temperature. Limnol. Oceanogr. **43**: 679–694. doi:10.4319/lo.1998.43.4.0679

Grossowicz, M., D. Roth-Rosenberg, D. Aharonovich, J. Silverman, M. J. Follows, and D. Sher. In press. *Prochlorococcus* in the lab and in silico: The importance of representing exudation. Limnol. Oceanogr.

Hemmings, J. C. P., M. Barciela, and M. J. Bell. 2008. Ocean color data assimilation with material conservation for improving model estimates of air-sea CO2 flux. J. Mar. Res. **66**: 87–126. doi:10.1357/002224008784815739

Hitchcock, G. L. 1980. Influence of temperature on the growth rate of *Skeletonema costatum* in response to variations in daily light intensity. Mar. Biol. **57**: 261–269. doi:10.1007/BF00387569

Hobson, L. A., F. A. Hartley, and D. E Ketcham 1979. Effects of variation in daylength and temperature on net rates of photosynthesis, dark respiration, and excretion by Isochrysis galbana Parke. Plant Physiology **63**: 947–951.

Karl, D. M., and others. 2003. Temporal studies of biogeochemical processes determined from ocean time-series observations during the JGOFS era. *In* M. J. R. Fasham [ed.], Ocean biogeochemistry. Springer.

Kepkay, P. E., F. Jellett, and S. E. H. Niven. 1997. Respiration and the carbon-to-nitrogen ratio of a phytoplankton bloom. Mar. Ecol. Prog. Ser. **150**: 249–261. doi:10.3354/meps150249

Kooijman, S.A.L.M. 2010. Dynamic energy budget theory for metabolic organization. Cambridge Univ. Press.

Lignell, R., H. Haario, M. Laine, and T. F. Thingstad. 2013. Getting the "right" parameter values for models of the pelagic microbial food web. Limnol. Oceanogr. **58**: 301–313. doi:10.4319/lo.2013.58.1.0301

Löptien, U., and H. Dietze. 2015. Constraining parameters in marine pelagic ecosystem models–is it actually feasible with typical observations of standing stocks? Ocean Sci. **11**: 573–590. doi:10.5194/os-11-573-2015

Metropolis, N., A. W. Rosenbluth, M. N. Rosenbluth, A. H. Teller, and E. Teller. 1953. Equations of state calculations by fast computing machines. J. Chem. Phys. **21**: 1087–1092. doi:10.1063/1.1699114

Mooshammer, M., and others. 2014. Adjustment of microbial nitrogen use efficiency to carbon:nitrogen imbalances regulates soil nitrogen cycling. Nat. Commun. **5**: 3694. doi:10.1038/ncomms4694

Myklestad, S. M. 1995. Release of extracellular products by phytoplankton with special emphasis on polysaccharides. Sci. Total Environ. **165**: 155–164. doi:10.1016/0048-9697(95)04549-G

Omta, A. W., J. Bruggeman, S.A.L.M. Kooijman, and H. A. Dijkstra. 2006. The biological carbon pump revisited: Feedback mechanisms between climate and the Redfield ratio. Geophys. Res. Lett. **33**: L14.613. doi:10.1029/2006GL026213

Omta, A. W., J. Bruggeman, S.A.L.M. Kooijman, and H. A. Dijkstra. 2009. The organic carbon pump in the Atlantic. J. Sea Res. **62**: 179–187. doi:10.1016/j.seares.2009.06.005

Partensky, F., W. R. Hess, and D. Vaulot. 1999. *Prochlorococcus*, a marine photosynthetic prokaryote of global significance. Microbiol. Mol. Biol. Rev. **63**: 106–127.

Rappe, M. S., A. Connon, K. L. Vergin, and S. J. Giovannoni. 2002. Cultivation of the ubiquitous SAR11 marine bacterioplankton clade. Nature **418**: 630–633. doi:10.1038/nature00917

Riper, D. M., G. Owens, and P. G. Falkowski. 1979. Chlorophyll turnover in *Skeletonema costatum*, a marine plankton diatom. Plant Physiol. **64**: 49–54. doi:10.1104/pp.64.1.49

Romera-Castillo, C., H. Sarmento, X. A. Alvarez-Salgado, J. M. Gasol, and C. Marrase. 2010. Production of chromophoric dissolved organic matter by marine phytoplankton. Limnol. Oceanogr. **55**: 446–454. doi:10.4319/lo.2010.55.1.0446

Ross, O. N., and R. J. Geider. 2009. New cell-based model of photosynthesis and photo-acclimation: Accumulation and mobilization of energy reserves in phytoplankton. Mar. Ecol. Prog. Ser. **383**: 53–71. doi:10.3354/meps07961

Smith, S. L., E. Casareto, M. P. Niraula, Y. Suzuki, J. C. Hargreaves, J. D. Annan, and Y. Yamanaka. 2007.

Examining the regeneration of nitrogen by assimilating data from incubations into a multi-element ecosystem model. J. Mar. Syst. **64**: 135–152. doi:10.1016/j.jmarsys.2006.03.013

Smith, S. L., and Y. Yamanaka. 2007. Quantitative comparison of photoacclimation models for marine phytoplankton. Ecol. Modell. **201**: 547–552. doi:10.1016/j.ecolmodel.2006.09.016

Suratman, S., K. Weston, T. Jickells, R. Chance, and T. Bell. 2008. Dissolved organic matter release by an axenic culture of *Emiliania huxleyi*. J. Mar. Biol. Assoc. UK **88**: 1343–1346. doi:10.1017/S0025315408002026

Thornton, D. C. O. 2014. Dissolved organic matter (DOM) release by phytoplankton in the contemporary and future ocean. Eur. J. Phycol. **49**: 20–46. doi:10.1080/09670262.2013.875596

Vallina, S. M., J. Follows, S. Dutkiewicz, J. M. Montoya, P. Cermeno, and M. Loreau. 2014. Global relationship between phytoplankton diversity and productivity in the ocean. Nat. Commun. **5**: 4299. doi:10.1038/ncomms5299

Volk, T., and M. I. Hoffert. 1985. Ocean carbon pumps: Analysis of relative strengths and efficiencies in ocean-driven atmospheric CO2, p. 99–110. *In* E. T. Sundquist and W. S. Broecker [eds.], The carbon cycle and atmospheric CO2: Natural variations Archean to present. AGU.

Weger, H. G., G. Birch, I. R. Elrifi, and D. H. Turpin. 1988. Ammonium assimilation requires mitochondrial respiration in the light: A study with the green alga *Selenastrum minutum*. Plant Physiol. **86**: 688–692. doi:10.1104/pp.86.3.688

Zlotnik, I., and Z. Dubinsky. 1989. The effect of light and temperature on DOC excretion by phytoplankton. Limnol. Oceanogr. **34**: 831–839. doi:10.4319/lo.1989.34.5.0831

Conflict of Interest

None declared.

Associate editor: Tammi Richardson